

Co-Crystallization of Sym-Triiodo-Trifluorobenzene with Bipyridyl Donors: Consistent Formation of Two Instead of Anticipated Three N⋯I Halogen Bonds

André C. B. Lucassen,[†] Amir Karton,[†] Gregory Leitus,[‡] Linda J. W. Shimon,[‡] Jan M. L. Martin,[†] and Milko E. van der Boom^{*,†}

Departments of Organic Chemistry and Chemical Research Support, The Weizmann Institute of Science, 76100 Rehovot, Israel

Received October 18, 2006

ABSTRACT: The potential triple-halogen-bond acceptor, sym-triiodo-trifluorobenzene IFB (**1**), has been co-crystallized with a series of bipyridyl derivatives (**2–4**) to gain insight to the factors controlling formation of multiple halogen bonds with a single aromatic system. Co-crystals **5–7** were obtained that consistently contained two N⋯I halogen bonds. The reluctance to the formation of a supramolecular assembly having a third N⋯I halogen bond does not depend on the size of the bispyridine donor systems (**2–4**). Apparently, there are limitations to the number of halogen bonds that can be formed with a single aromatic halogen donor. The solid-state structure of co-crystal (**5**) contains short I⋯F contacts of 2.96 and 3.05 Å. DFT calculations were performed at the PBE0/(apc1-aSDBDZ)//PBE0/(pc1-SDBDZ) level of theory to investigate the nature of the interaction between the pyridine nitrogen and IFB (**1**). These calculations reveal a weakening of N⋯I interactions as more pyridine moieties coordinate to the IFB (**1**), which might be a contributing factor to the consistent formation of two rather than three N⋯I halogen bonds.

Introduction

Halogen bonding involves an interaction in which a halogen atom (Cl, Br, I) acts as an acceptor for lone-pair electrons of a heteroatom (N, O, S, P). Halogen and hydrogen bonding have somewhat analogous characteristics in terms of directionality and $n \rightarrow \sigma^*$ donor–acceptor interactions. Perfluorination of an iodo/bromo-hydrocarbon results in enhanced acceptor ability, and the interactions become comparable to, or even dominate over, hydrogen bonding.¹ Its use in co-crystallization and solid-state reactivity has been demonstrated in recent years by the groups of Resnati, Hanks, and others.^{2–7} Examples of halogen bonding as a tool for the formation of liquid crystals show its potential for the development of new materials.^{8,9} Nevertheless, the number of new derivatives prepared for halogen-bonding studies (especially fluorinated examples) is relatively small compared to the growing number of hydrogen-bonded supramolecular systems. In addition, several theoretical investigations on halogen bonding have been reported.^{10–14} Clearly, there is ample opportunity for the design of new molecular building blocks for halogen bonding applications in many different fields, ranging from liquid crystals to enzyme–substrate interactions.¹⁵ We have recently reported on the preparation and solution and solid-state properties of a stilbazole derivative that combines halogen-bonding donor and acceptor sides in the same fluorinated chromophore.¹⁶ Compounds combining halogen donor and acceptor sites are rare.^{17–19} Remarkably, no halogen-bonding studies for trigonal fluorinated halobenzenes have been reported, in sharp contrast with the wealth of somewhat analogous trigonal building blocks available for supramolecular synthesis using hydrogen bonding.^{20–27} Trigonal molecular building blocks like 1,3,5-cyclohexane tricarboxylic acid, 1,3,5-benzenetricarboxylic acid (trimesic acid), and similar derivatives have proven extremely fruitful crystallization partners in the engineering of supramolecular structures through hydrogen bonding.^{20–28} Their

co-crystallization with bispyridine derivatives is well-studied and leads to hexagonal networks that can exhibit complex interpenetration.^{20,21,29,30} We envisaged 1,3,5-triiodo-2,4,6-trifluorobenzene (**1**) (IFB)^{31,32} as an ideal candidate, because the relatively electron-poor iodine atoms in IFB (**1**) should be good electron acceptors for halogen bonding with, for example, nitrogen-containing donor molecules (Scheme 1). Both 1,4- and 1,3-diiodo-tetrafluorobenzene form co-crystals with bipyridyl derivatives.¹⁵ Packing effects play an important role in the formation of halogen-bonded supramolecular assemblies, as they may favor a linear arrangement of pyridyl groups, to fill space without requiring interpenetrating halogen-bonded networks. Furthermore, π -stacking/aggregation of chromophores such as bis-1,4-(4-pyridylethyl-enyl)-benzene (BPEB, **2**), *trans*-1,2-di-(4-pyridyl)-ethylene (DPE, **3**), and 4,4'-bipyridine (BiPy, **4**) in the solid state might be affected by stacking interactions with IFB (**1**).^{5,33} DFT calculations were performed to evaluate the additive effect of pyridine donors on the strength of the N⋯I interactions. Weakening of the halogen bond occurs as more pyridines coordinate to the IFB (**1**), which may contribute to the experimental findings that the number of halogen-bond interactions on an aromatic acceptor is limited.

Results and Discussion

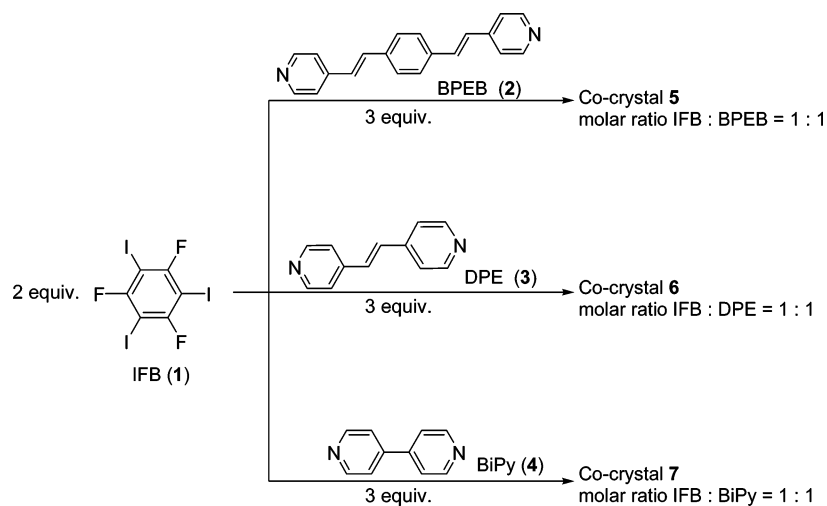
The results obtained from the co-crystallizations of IFB (**1**) with bipyridines **2–4** are summarized in Scheme 1 and Tables 1 and 2.

Slow evaporation of a chloroform solution at room temperature containing IFB (**1**) and BPEB (**2**) in a 2:3 molar ratio gave light yellow crystals suitable for X-ray crystallography. The co-crystal structure **5** has two N⋯I halogen bonds (Figure 1). Compounds **1** and **2** co-crystallize preferably in a 1:1 molar ratio instead of the anticipated 2:3 ratio, as might be expected for a system having three possible sites for iodine⋯pyridine–nitrogen interactions. Co-crystallization of compound **1** with 3 equiv of BPEB (**2**) resulted again in the 1:1 co-crystal **5**. The excess BPEB (**2**) precipitated as an amorphous powder after the formation of co-crystals **5**.

* Corresponding author. E-mail: milko.vanderboom@weizmann.ac.il.

[†] Department of Organic Chemistry, The Weizmann Institute of Science.

[‡] Department of Chemical Research Support, The Weizmann Institute of Science.

Scheme 1. Co-crystallizations of IFB (1) with Bipyridyl Derivatives 2–4.^a

^a Compounds were mixed in a 2:3 Molar Ratio in chloroform at room temperature. Applying a 1:3 ratio of compounds **1** and **2** also resulted in co-crystal **5**.

Table 1. Compound 1 and Co-Crystals 5–7 with Selected Angles, Intramolecular Distances, and Classification

compd	molar ratio	observed molar ratio	solvent, concentration	N···I dist. (Å)	C–I···N angles (deg)	I···I dist. (Å) (contact type)	I···F dist. (Å) (contact type)	stacking dist. (Å)
IFB (1) ^a			hexane			3.746(1) (II)	3.556(3)	3.54(5)
BPEB (2)	2:3 and 1:3	5 (1:1)	CHCl ₃ , 20 mM	2.829(3) 2.928(3) 2.799(3) 2.961(3)	165.4(2) 167.2(2) 173.2(1) 160.6(1)	not relevant ^b	2.942(3) (I) 3.051(2) (I)	3.45(6) 2 3.60(5) 1
DPE (3)	2:3	6 (1:1)	CHCl ₃ , 20 mM	2.821(7) 2.846(7)	173.9(3) 171.1(3)	not relevant ^b	3.483(4) ^c	3.58(6)
BiPy (4)	2:3	7 (1:1)	CHCl ₃ , 40 mM	2.841(1) 2.94(2)	171.5 164.7	not relevant ^b	3.149(9) (I)	3.80(2) 4 3.55(1) 1

^a See the Supporting Information for details. ^b I···I distances between stacked molecules **1**, classification not applicable. ^c From the angles θ_1 (124.5° resp 136.9°) and θ_2 (144.6° resp 139.1°), this would be type I contacts, but the I···F distances of 3.56 and 3.48 Å for compound **1** and co-crystal **6**, respectively, are larger than the sum of van der Waals radii. The 3.45 Å type II contact ($\theta_1 = 73.0^\circ$, $\theta_2 = 165.0^\circ$) of **1** is exactly the sum of the van der Waals radii.

Table 2. Selected Bond Lengths (*R*, in Å) of IFB (1) and Assemblies 8–10 Calculated at the PBE0/pc1-SDBDZ Level of Theory

		IFB	8	9	10
C–I	<i>r</i> ₁	2.093	2.123	2.121	2.119
	<i>r</i> ₂	2.093	2.096	2.121	2.119
	<i>r</i> ₃	2.093	2.096	2.097	2.119
I···N	<i>r</i> ₄		2.791	2.822	2.852
	<i>r</i> ₅			2.822	2.852
	<i>r</i> ₆				2.853
					2.853

The crystal structure of co-crystals **5** relates to a monoclinic spacegroup *P2/c* (No. 13). The unit cell contains two half IFB (**1**) molecules on a 2-fold rotation axis, one in a general position, two half BPEB (**2**) molecules on an inversion center, and one in a general position. The unit-cell dimensions are 18.066(4), 9.135(2), and 31.410(6) Å for the *a*, *b*, and *c* axes, respectively. Molecules **2** are arranged in a herringbone-type fashion (along the *a* axis), separated by layers of molecule **1**. Both nitrogen atoms of compound **2** are involved in N···I halogen bonding in the *a*–*c* plane of the crystal lattice. Two different interacting IFB (**1**) and BPEB (**2**) pairs exist in the co-crystal; one pair has N···I distances of 2.829(3) and 2.928(3) Å (C–I···N angles 165.4(2) and 167.2(2)°, respectively), whereas the second IFB (**1**) and BPEB (**2**) couple has N···I distances of 2.799(3) and 2.961(3) Å, respectively (with C–I···N angles of 173.2(1) and 160.6(1)°, respectively). These distances are 16–20% shorter than the sum of the van der Waals radii (3.51 Å), which is in good agreement with other N···I halogen bonds.^{2,15} The distances of 3.45(6) and 3.60(5) Å between two molecules of **2**

point to significant stabilization by π -stacking interactions. Another view of the overall structure of **5** is shown in Figure 2, where compounds **1** and **2** are categorized by symmetry equivalence. Both compounds **1** and **2** are divided into three groups, meaning that each molecule has three symmetry-unrelated molecules in the asymmetric unit (in accordance with a *Z* value of 8).

The IFB molecules **1** are aligned in a face-to-face orientation along the *a* axis and an edge-to-edge orientation along the *b* axis. As symmetry-nonequivalent molecules are lying face to face, the alignment is not perfectly columnar but shows a slippage; this is in contrast with structures **6** and **7**, in which alignment is perfect (vide infra). The edge-to-edge arrangement involves symmetry-equivalent molecules **1** and shows remarkably short I···F contacts of 2.962(3) and 3.051(2) Å (15 and 11% less than the sum of the van der Waals radii, 3.43 Å). These I···F contacts are also much shorter than the I···F contacts of 3.556(3) Å in the crystal structure of compound **1**. Although intermolecular halogen–halogen interactions are well-documented,³⁴ we found only three other examples of short, nonionic, I···F interactions in organic crystals.^{35–37} All of these I···F interactions occur in highly reactive compounds with hypervalent fluorinated iodine atoms, resulting in highly polarized structures and short intermolecular I···F contacts. Moreover, in co-crystal **5**, the angles θ_1 for C–I···F and θ_2 for I···C–F are equal, both being 180° for the I···F interactions with an intermolecular contact distance of 2.942(3) Å. The angles θ_1 and θ_2 are 162.1(1) and 162.3(2)° for the second contact with an intermolecular I···F distance of 3.051(2) Å.

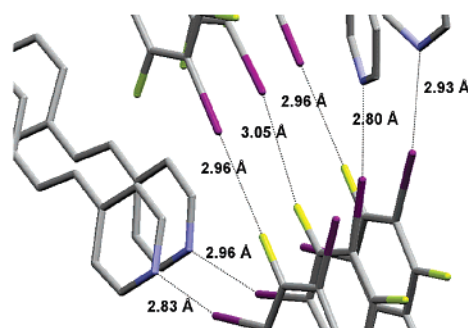
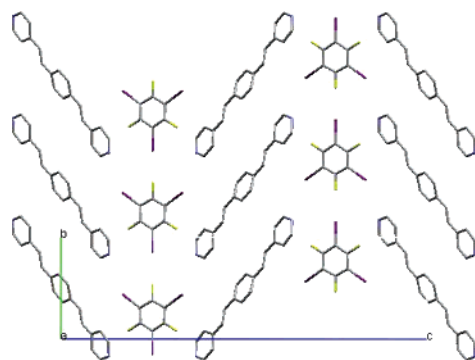


Figure 1. Crystal structure of co-crystal **5** illustrating the herringbone arrangement (left) and short N \cdots I and I \cdots F distances (right). Co-crystallizing either 2:3 or 1:3 molar ratios of IFB (**1**) and BPEB (**2**), respectively (from chloroform at room temperature), led to the same structure **5** with a 1:1 molar ratio. Colors: carbon, gray; nitrogen, blue; fluorine, yellow; iodine, purple.

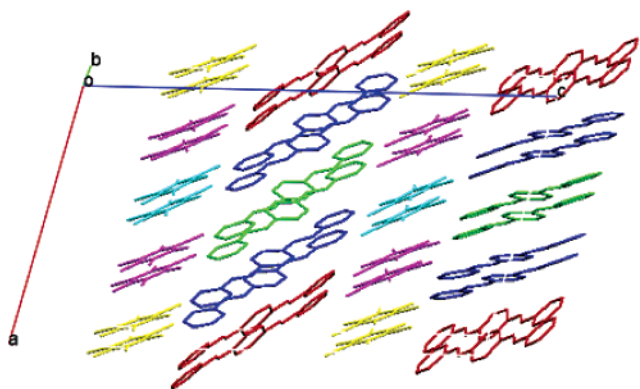


Figure 2. Crystal lattice of co-crystal **5** colored according to symmetry equivalence. Symmetry-equivalent molecules of compounds **1** and **2** are shown in the same color. Along the stacking direction, an A–B–C–B pattern is apparent. Note the twist in orientation of symmetry-nonequivalent molecule **2** in the “stacks”.

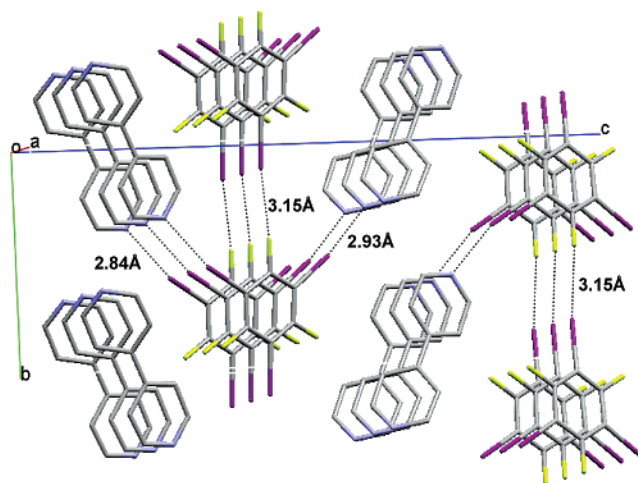


Figure 4. View of 1:1 co-crystal **7** with two intermolecular N \cdots I halogen bonds of 2.84(1) and 2.94(2) Å. The intermolecular I \cdots F distance of 3.149(9) Å is somewhat longer compared to those found in co-crystal **5**. Co-crystals **7** were obtained by slow evaporation of a chloroform solution of compounds **1** and **4** with a 2:3 molar ratio at room temperature. View along the *a*-axis. Colors: carbon, gray; nitrogen, blue; fluorine, yellow; iodine, purple.

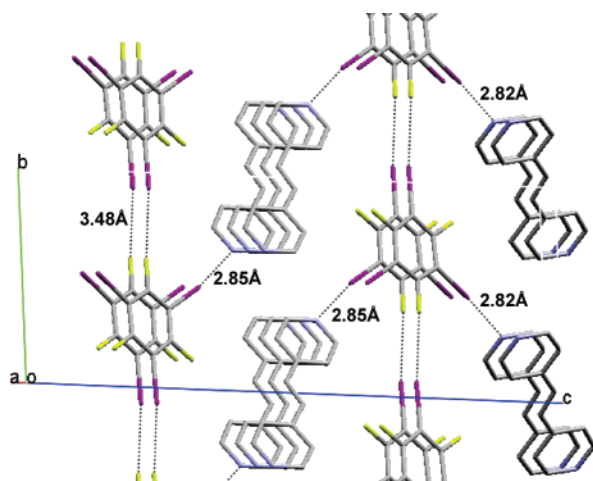


Figure 3. View of 1:1 co-crystal **6** with the two N \cdots I halogen bonds of 2.821(7) and 2.846(7) Å. Note that the intermolecular I \cdots F distance is much longer (3.483(4) Å) compared to those found in co-crystal **5** (2.942(3) and 3.051(2) Å). Co-crystals **6** were prepared by slow evaporation at room temperature of a chloroform solution of IFB (**1**) and DPE (**3**) with a 2:3 molar ratio. Colors: carbon, gray; nitrogen, blue; fluorine, yellow; iodine, purple.

Halogen–halogen interactions have been divided into two categories depending on the two angles of the C–X₁⋯X₂–C contact.^{32,34,38–42} Type I contacts were defined as having equal angles $\theta_1(\text{C–X}_1\cdots\text{X}_2)$ and $\theta_2(\text{C–X}_2\cdots\text{X}_1)$. In type II contacts, $\theta_1 = 180^\circ$ and $\theta_2 = 90^\circ$ where, if $\text{X}_1 \neq \text{X}_2$, the heavier (more

polarizable) halogen is usually X₁. According to the above definition, a type I contact is nonstabilizing and a consequence of crystallographic symmetry (the X atoms located across a center of inversion), whereas a type II contact involves interaction between the oppositely polarized regions of atoms X₁ and X₂ and has a stabilizing effect. Thus, according to the abovementioned classification by Desiraju and Parthasarathy,^{32,34,38–42} the I \cdots F contacts in co-crystal **5** are pure type I nonstabilizing interactions and a result of symmetry in the crystal. Pure type I contacts for unsymmetrical halogen–halogen interactions, especially for I \cdots F contacts, where the difference in polarizability is at its maximum, should be highly unlikely, “barring a fortuitous equality of angles.”³⁴

Mixing chloroform solutions of compound **1** and bis(4-pyridyl)-ethylene (DPE) (**3**) in a 2:3 molar ratio at concentrations above 50 mM resulted in immediate precipitation of a white microcrystalline solid. Crystallization began nearly instantly when more dilute chloroform solutions (e.g., 20 mM) of compounds **1** and **3** were mixed at room temperature, resulting in the formation of white X-ray quality crystals. Co-crystal **6** (spacegroup $P\bar{1}$, triclinic) again had a 1:1 molar ratio (instead of 2:3), analogous to co-crystal **5** with only two of the three iodine atoms involved in a N \cdots I halogen bond with DPE (**3**)

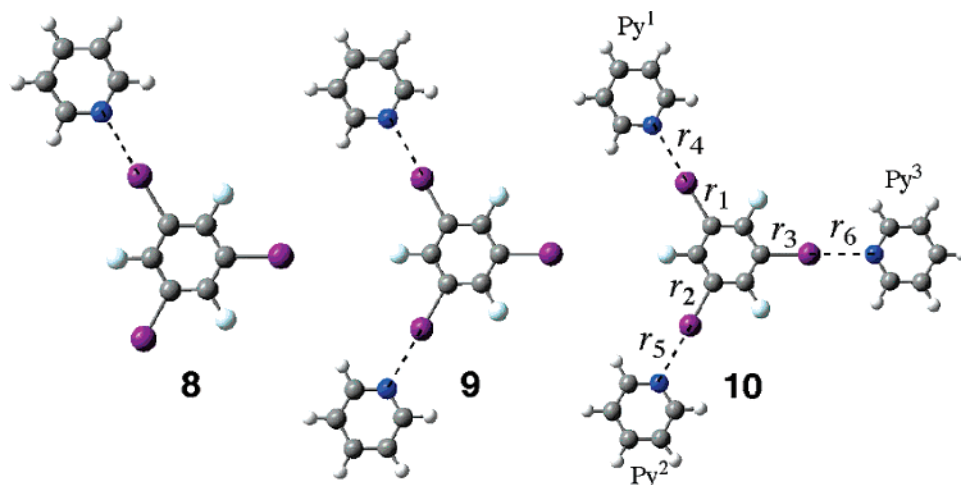


Figure 5. Optimized geometries of **8–10** calculated at the PBE0/(pc1-SDBDZ) level of theory. The bond numbering scheme (r) used is shown (see Table 2). (Atomic color scheme: C, green; H, white; N, blue; F, turquoise; I, purple.)

Table 3. Complexation Energy (ΔE , in kcal/mol) and Counterpoise Corrected Complexation Energy (ΔE^{CP}) of the n th Pyridine (Py) to IFB(pyridine) $_{n-1}$, Calculated at the PBE0/(apc1-aSDBDZ)//PBE0/(pc1-SDBDZ) Level of Theory

n	$-\Delta E$	$-\Delta E^{\text{CP}}$
1 (8)	7.127	5.840
2 (9)	6.092	4.868
3 (10)	5.351	4.172

Table 4. Overall APT Charge Transferred (in me) from the Pyridine Molecules to the IFB (**1**) upon Complexation Calculated at the PBE0/(apc1-aSDBDZ)//PBE0/(pc1-SDBDZ) Level of Theory

	8	9	10
Py ¹	64.5	57.7	51.6
Py ²		57.7	51.6
Py ³			51.1

(Figures 2 and 3). The values of the N \cdots I contacts are typical, 2.821(7) and 2.846(7) Å, with C–I \cdots N angles of 173.9(3) and 171.1(3)°, respectively. In contrast to the structure of co-crystal **5**, in co-crystal **6**, the asymmetric unit contains only symmetry-related molecules of **1** and **3**. The I \cdots F distance of 3.483(4) Å involving the third iodine atom is substantially longer (approximately 0.5 Å) than the I \cdots F-distance observed in co-crystal **5**. The stacking distance of 3.58(6) Å between the stacked molecules **1** and **3** again implies stabilization through π – π -stacking.

Co-crystals **7** were obtained by slow evaporation of a chloroform solution of **1** and BiPy (**4**) in the molar ratio 2:3 at room temperature (Figure 4). Similar to co-crystals **5** and **6**, co-crystal **7** has a 1:1 molar ratio and only two of the three possible N \cdots I halogen bonds (2.84(1), 2.94(2) Å) and C–I \cdots N angles of 171.5 and 164.7°, respectively. The unit cell of co-crystal **7** contains only symmetry-related molecules of IFB (**1**) and 4,4'-bipyridine (**4**), respectively, which is similar to co-crystal **6**. The stacking distance of 3.55(1) Å between units **1** is comparable to the values for co-crystals **5** and **6** (3.45(6) and 3.60(5) Å, respectively). However, the stacking distance between the 4,4'-bipyridine molecules (**4**) of 3.80(2) Å is somewhat larger. It should be noted that compound **2** has a limited solubility in chloroform, so a lower concentration (max. 20 mM) had to be used to prepare co-crystals **5**. The solubility of compounds **1**, **3**, and **4** in chloroform is very good (>300 mM) and much better than that of the resulting co-crystals **6** and **7**.

Table 5. Perturbation Energy $E(2)$ (in kcal/mol) and Corresponding Orbital Occupancies

		$E(2)$	occupancy of N σ -lone pair orbital	occupancy of C–I σ^* orbital
8	C–I \cdots Py ¹	8.20	1.8663	0.0854
	C–I			0.0301
	C–I			0.0301
9	C–I \cdots Py ¹	8.15	1.8720	0.0827
	C–I \cdots Py ²	8.15	1.8720	0.0827
	C–I			0.0300
10	C–I \cdots Py ¹	7.41	1.8768	0.0785
	C–I \cdots Py ²	7.41	1.8768	0.0785
	C–I \cdots Py ³	6.84	1.8770	0.0763

The main characteristics regarding the short intermolecular contacts with distance angles of co-crystals **5–7** are given in Table 1.

As can be seen from Table 1, both the stacking distances between the aromatic systems and the I \cdots F distances vary for co-crystals **5–7**. However, there seems to be no apparent correlation between the size/length of the bipyridine derivative and these distances.

Density Functional Calculations. DFT calculations were performed to further investigate the nature of the interaction between the pyridine nitrogen and the Ar_F–I moiety. For reasons of computational cost, the bipyridyl ligands (**2–4**) were substituted by pyridine. The complex geometries calculated at the PBE0/(pc1-SDBDZ) level of theory are shown in Figure 5. Table 2 lists selected equilibrium bond lengths for IFB (**1**) and for three IFB–(pyridine) $_n$ ($n = 1–3$) assemblies (**8–10**). The calculated bond lengths of IFB (**1**) and IFB–(pyridine) $_2$ (**9**) are in good agreement with the corresponding crystal structures **5–7**. Upon complexation, the C–I bond is lengthened by 0.030, 0.028, and 0.026 Å for **8–10**, respectively. These elongations are consistent with the weakening of the C–I bond due to the interaction of the nitrogen lone pair with the lowest vacant σ^* orbital of C–I. The C–I bond involved in the I \cdots N interaction is shortened (by 0.002 Å) and the I \cdots N halogen bond is lengthened (by 0.03 Å) each time another pyridine unit is introduced into the system. These trends demonstrate the weakening of the I \cdots N halogen bond as more pyridines coordinate to the IFB. Table 3 gives the I \cdots N binding energy (ΔE) and the counterpoise (CP) corrected binding energy (ΔE^{CP}), i.e., the complexation energy of IFB \rightarrow **8**, **8** \rightarrow **9**, and **9** \rightarrow **10**. The ΔE^{CP} of the formation of **8** (5.84 kcal/mol) is typical for such types of halogen bonding. For instance, the

Table 6. Crystallographic Data for Compound **1** and Co-Crystals **5–7**

	compd 1	co-crystal 5	co-crystal 6	co-crystal 7
formula	C ₆ I ₃ F ₃	C ₂₆ H ₁₆ F ₃ I ₃ N ₂	C ₁₈ H ₁₀ F ₃ I ₃ N ₂	C ₁₆ H ₈ F ₃ I ₃ N ₂
molar mass (g mol ⁻¹)	509.76	794.13	691.98	665.94
cryst color	white	yellow	white	white
cryst dimensions (mm ³)	1.0 × 0.1 × 0.1	1.0 × 0.1 × 0.05	0.6 × 0.1 × 0.1	1.0 × 0.5 × 0.2
cryst syst	monoclinic	monoclinic	triclinic	monoclinic
space group	<i>P</i> 2 ₁ / <i>n</i>	<i>P</i> 2/ <i>c</i>	<i>P</i> 1	<i>P</i> <i>n</i>
<i>a</i> (Å)	13.818(3)	18.066(4)	4.7330(9)	4.0830(8)
<i>b</i> (Å)	4.758(1)	9.135(2)	9.065(2)	9.056(2)
<i>c</i> (Å)	15.385(3)	31.410(6)	22.598(4)	24.046(5)
α (deg)	90	90	94.53(3)	90
β (deg)	107.08(3)	105.07(3)	93.22(3)	92.17(3)
γ (deg)	90	90	92.32(3)	90
<i>Z</i>	4	8	2	2
<i>V</i> (Å ³)	966.9(3)	5005.4(18)	964.0(3)	888.5(3)
ρ _{calcd} (mg m ⁻³)	3.502	2.108	2.384	2.489
no. of unique data	1317	11417	2268	1611
<i>R</i> ₁	0.0165	0.0376	0.0341	0.0434
<i>wR</i> ₂	0.0415	0.0708	0.0643	0.1132
GOF (<i>F</i> ²)	1.118	1.015	1.057	1.051

experimental enthalpy of formation of a complex between CF₃I and 2,4,6-trimethylpyridine is 5.0 kcal/mol.⁴³ The Δ*E*^{CP} of the formation of **9** and **10** is lower by 0.97 and 1.67 kcal/mol, respectively. Table 4 summarizes the overall APT charge transferred (*Q*_{CT}) from each pyridine unit to the IFB molecule upon complexation. *Q*_{CT} is reduced with an increasing number of pyridines bound to the IFB, which is in line with the calculated trends for the bond lengths and complexation energies. The squared correlation coefficient between the Δ*E* or Δ*E*^{CP} and *Q*_{CT} is 0.996, suggesting that charge-transfer interactions play an important role in the formation of I⋯N halogen bonds. The donor–acceptor stabilization energy for each of the I⋯N bonds may be approximated by the second-order perturbation energy *E*(2) obtained from natural bond orbital (NBO) analysis.⁴⁴ Table 5 lists *E*(2) and the corresponding orbital occupancies. *E*(2) is in accordance with the trend of general reduction in the I⋯N binding energy as more pyridines are coordinated to the IFB (i.e., 8.20, 8.15, and 7.41 kcal/mol for **8–10**, respectively). For **10**, which belongs to the *C*2 point group (see computational details), both *Q*_{CT} and *E*(2) suggest that the I⋯N bond parallel to the *C*2 axis (i.e., IFB⋯Py³) is slightly weaker than the other two halogen bonds.

Summary and Conclusions

Co-crystallization of IFB (**1**) with a series of three different bipyridyl derivatives (**2–4**) in a 2:3 molar ratio (or a 1:3 ratio as verified for BPEB (**2**)) consequently yields 1:1 co-crystals with only two N⋯I halogen bonds. Apparently, this arrangement is preferable in this system over the formation of a crystal lattice with 3-fold I⋯N intermolecular interactions. Three-fold intermolecular motifs are common with hydrogen-bonded systems.^{20,21,30} Packing constraints seem to dominate over the possibility of the formation of a third N⋯I halogen bond and do not seem to be affected by the size of the bipyridyl donors. The observed stoichiometry might be due to packing effects that favor chain formation over 2D open layers, because this would require extensive interpenetration to fill space. As close packing is driven by a gain in enthalpy,⁴⁰ this gain is obviously larger than the benefit from a third halogen bond. Alternatively, donation of charge to compound **1** resulting from two halogen bonds may have a detrimental effect on the capacity of the third iodine atom bound to the same aromatic system to act as an acceptor for another halogen bond. Indeed, DFT calculations using a model system support this hypothesis.

In conclusion, we have shown that 1,3,5-triiodo-2,4,6-trifluorobenzene (IFB, **1**) readily forms co-crystals with bipyridyl-

type donors through halogen bonding. Halogen-bonded systems have been compared with hydrogen-bonded systems in terms of strength and directionality;¹ however, a 3-fold in-plane intermolecular halogen-bonding interaction with one aromatic system remains of yet elusive.

Experimental Section

Chloroform (Biolab, AR) was passed over a column of basic alumina (grade 1) and stored over 4 Å molecular sieves. Hexane (Biolab, AR) was distilled from calcium hydride under a nitrogen atmosphere. Bis-1,4-(4-pyridylethynyl)-benzene BPEB (**2**) was prepared according to a literature procedure,⁴⁵ *trans*-1,2-di(4-pyridyl)-ethylene (97%) DPE (**3**) and 4,4'-bipyridyl (>99%) (**4**) were obtained from Fluka and Aldrich, respectively, and used as received.

1,3,5-Triiodo-2,4,6-trifluorobenzene (1). This compound was prepared by iodination of 1,3,5-trifluorobenzene according to a literature procedure.³¹ Suitable crystals for X-ray crystal structure determination (small white needles, 1.0 × 0.1 × 0.1 mm³) were obtained by recrystallization from hexane, cooling a warm (50 °C) solution slowly to room temperature overnight (see Table 6 and the Supporting Information).³² No suitable crystals of **1** were obtained from chloroform because of its high solubility in this solvent.

Preparation of Co-Crystals (5–7). Co-crystal **5**: A solution of **1** (0.13 mmol) in chloroform (2 mL) was added to a chloroform solution (8 mL) of **2** (0.20 mmol) in a 20 mL screw-capped vial at room temperature. The vial was kept in the dark, and the chloroform was allowed to evaporate slowly until, after formation of light yellow co-crystals **5**, excess **2** started to precipitate out of the solution. In several cases, all chloroform was allowed to evaporate and the precipitating solid was shown to be pure **2** as judged by ¹H NMR. Co-crystals **6** and **7** were prepared analogously. In the case of co-crystal **6**, the concentrations of compounds **1** and **3** were kept below 50 mM to avoid immediate precipitation of the co-crystals, which made it difficult to obtain specimens suitable for X-ray experiments. Relevant crystallographic data for compound **1** and co-crystals **5–7** are summarized in Table 2.

X-ray Data Collection and Processing. Data were collected at 120 K on a Nonius KappaCCD diffractometer, Mo Kα (λ = 0.71073 Å), graphite monochromator. The data were processed with Denzo-scalepack. Solution and refinement: Structures were solved by direct methods with SHELXS. Full matrix least-squares refinement on the basis of *F*² with SHELXS-97. Refinement of *F*² was against all reflections. Stacking distances were determined by calculating the best plane through a ring and subsequent determination of the distance of the ring atoms of the neighboring molecule and averaging of these distances. Crystallographic data for compound **1** and co-crystals **5–7** are listed in Table 6. The X-ray structure of compound **1** has been reported,³² but has been remeasured and included in Table 6 for comparison (see the Supporting Information).

Computational Details. All calculations were carried out using Gaussian 03, revision C.01.⁴⁶ The PBE0 DFT exchange-correlation functional was used for the investigation.⁴⁷ This functional is the hybrid variant (25% HF exchange) of PBE (Perdew, Burke, and Ernzerhof's)⁴⁸

nonempirical GGA functional. With this functional, two basis set–RECP (relativistic effective core potential) combinations were used. The first, denoted pc1-SDBDZ, is the combination of the Jensen's polarization consistent double- ζ basis set (pc1)⁴⁹ on lighter elements with the Stuttgart–Dresden basis set–RECP⁵⁰ on iodine. The second, denoted apc1-aSDBDZ, corresponds to the augmented versions of the pc1⁴⁹ and SDBDZ⁵¹ basis sets. Geometries were optimized using the former basis set, whereas the binding energies, BSSE corrections, and NBO analysis were calculated with the latter basis set; this level of theory is conventionally denoted as PBE0/apc1-aSDBDZ//PBE0/pc1-SDBDZ. Geometry optimizations were carried out using the default pruned (75,302) grid and with the highest possible symmetry constraints. In the case of **9** and **10** (Figure 5), however, small imaginary frequencies corresponding to the rotation of the pyridines around the weak I \cdots N interactions were obtained even with the “ultrafine” grid (i.e., a pruned (99 590) grid). These imaginary frequencies were eliminated when the symmetry constraints were reduced to the C₁ and C₂ point groups for **9** and **10**, respectively. The energies and NBO analysis were calculated with the “ultrafine” grid as recommended in the literature.⁵² In the single-point energy calculations of the larger systems **8**–**10**, the SCF convergence criterion was set to 10⁻⁶ a.u. For the calculation of the halogen bond energies, the basis set superposition error (BSSE) was taken into account using the counterpoise (CP) method.^{53,54} The donor–acceptor stabilization energies $E(2)$ were calculated by the second-order perturbation molecular orbital analysis using the NBO 5.0 program suite.⁵⁵

Acknowledgment. This research was supported by the Israel Science Foundation, MINERVA, Mordechai Glikson Fund, BMBF, and the MJRG for Molecular Materials and Interface Design. M.E.v.d.B. is the incumbent of the Dewey David Stone and Harry Levine career development chair. J.M.L.M. is the Baroness Thatcher Professor of Chemistry and a member ad personam of the Lise Meitner-Minerva Center for Computational Quantum Chemistry.

Supporting Information Available: The supplementary crystallographic data for this paper includes: (i) the crystallographic information files (CIF) for compound **1** and co-crystals **5**–**7**, (ii) the packing of compound **1** (Figure S1), (iii) and details regarding the solid-state structure of compound **1**. This material is available free of charge via the Internet at <http://pubs.acs.org>.

References

- Corradi, E.; Meille, S. V.; Messina, M. T.; Metrangolo, P.; Resnati, G. *Angew. Chem., Int. Ed.* **2000**, *39*, 1782.
- Metrangolo, P.; Resnati, G. *Chem.—Eur. J.* **2001**, *7*, 2511.
- Goroff, N. S.; Curtis, S. M.; Webb, J. A.; Fowler, F. W.; Lauher, J. W. *Org. Lett.* **2005**, *7*, 1891.
- Caronna, T.; Liantonio, R.; Logothetis, T. A.; Metrangolo, P.; Pilati, T.; Resnati, G. *J. Am. Chem. Soc.* **2004**, *126*, 4500.
- Crihfield, A.; Hartwell, J.; Phelps, D.; Walsh, R. B.; Harris, J. L.; Payne, J. F.; Pennington, W. T.; Hanks, T. W. *Cryst. Growth Des.* **2003**, *3*, 313.
- Syssa-Magalé, J. L.; Boubekeur, K.; Palvadeau, P.; Meerschaut, A.; Schollhorn, B. *CrystEngComm* **2005**, *7*, 302.
- Fourmigue, M.; Batail, P. *Chem. Rev.* **2004**, *104*, 5379.
- Nguyen, H. L.; Horton, P. N.; Hursthouse, M. B.; Legon, A. C.; Bruce, D. W. *J. Am. Chem. Soc.* **2004**, *126*, 16.
- Xu, J.; Liu, X.; Lin, T.; Huang, J.; He, C. *Macromolecules* **2005**, *38*, 3554.
- Valerio, G.; Raos, G.; Meille, S. V.; Metrangolo, P.; Resnati, G. *J. Phys. Chem. A* **2000**, *104*, 1617.
- Romaniello, P.; Lelj, F. *J. Phys. Chem. A* **2002**, *106*, 9114.
- Lommerse, J. P. M.; Stone, A. J.; Taylor, R.; Allen, F. H. *J. Am. Chem. Soc.* **1996**, *118*, 3108.
- Zou, J.-W.; Jian, Y.-J.; Guo, M.; Hu, G.-X.; Zhang, B.; H.-C., L.; Yu, Q.-S. *Chem.—Eur. J.* **2005**, *11*, 740.
- Ananthavel, S. P.; Manoharan, M. *Chem. Phys.* **2001**, *269*, 49.
- Metrangolo, P.; Neukirch, H.; Pilati, T.; Resnati, G. *Acc. Chem. Res.* **2005**, *38*, 386.
- Lucassen, A. C. B.; Vartanian, M.; Leitius, G.; van der Boom, M. E. *Cryst. Growth Des.* **2005**, *5*, 1671.
- Berski, S.; Ciunik, Z.; Drabent, K.; Latajka, Z.; Panek, J. *J. Phys. Chem. B* **2004**, *108*, 12327.
- Glaser, R.; Chen, N.; Wu, H.; Knotts, N.; Kaupp, M. *J. Am. Chem. Soc.* **2004**, *126*, 4412.
- Bond, A. D.; Griffiths, J.; Rawson, J. M.; Hulliger, J. *Chem. Commun.* **2001**, 2488.
- Bhogala, B. R.; Nangia, A. *Cryst. Growth Des.* **2003**, *3*, 547.
- Bhogala, B. R.; Basavoju, S.; Nangia, A. *Cryst. Growth Des.* **2005**, *5*, 1683.
- Wang, Z.; Kravtsov, V. C.; Zaworotko, M. J. *Angew. Chem., Int. Ed.* **2005**, *44*, 2877.
- Ahn, S.; PrakashaReddy, J.; Kariuki, B. M.; Chatterjee, S.; Ranganathan, A.; Pedireddi, V. R.; Rao, C. N. R.; Harris, K. D. M. *Chem.—Eur. J.* **2005**, *11*, 2433.
- Bushey, M. L.; Nguyen, T.-Q.; Zhang, W.; Horoszewski, D.; Nuckolls, C. *Angew. Chem., Int. Ed.* **2004**, *43*, 5446.
- Franz, A.; Bauer, W.; Hirsch, A. *Angew. Chem., Int. Ed.* **2005**, *44*, 1564.
- Ranganathan, A.; Pedireddi, V. R.; Rao, C. N. R. *J. Am. Chem. Soc.* **1999**, *121*, 1752.
- Wolff, J. J.; Gredel, F.; Oeser, T.; Irngartinger, H.; Pritzkow, H. *Chem.—Eur. J.* **1999**, *5*, 29.
- Maitra, U.; Balasubramanian, R. Some Aspects of Supramolecular Design of Organic Materials. In *Supramolecular Organization and Materials Design*; Jones, W., Rao, C. N. R., Eds.; Cambridge University Press: Cambridge, U.K., 2002; p 363.
- Krishnamohan Sharma, C. V.; Zaworotko, M. J. *Chem. Commun.* **1996**, 2655.
- Prins, L. J.; Reinhoudt, D. N.; Timmerman, P. *Angew. Chem., Int. Ed.* **2001**, *40*, 2382.
- Wenk, H. H.; Sander, W. *Eur. J. Org. Chem.* **2002**, 3927.
- Reddy, C. M.; Kirchner, M. T.; Gundakaram, R. C.; Padmanabhan, K. A.; Desiraju, G. R. *Eur. J. Chem.* **2006**, *12*, 2222.
- Shukla, A. D.; Strawser, D.; Lucassen, A. C. B.; Freeman, D.; Cohen, H.; Jose, D. A.; Das, A.; Evmenenko, G.; Dutta, P.; van der Boom, M. E. *J. Phys. Chem. B* **2004**, *108*, 17505.
- Pedireddi, V. R.; Reddy, D. S.; Goud, B. S.; Craig, D. C.; Rae, A. D.; Desiraju, G. R. *J. Chem. Soc., Perkin Trans. II* **1994**, 2353.
- Minkwitz, R.; Berkei, M. *Inorg. Chem.* **2001**, *40*, 36.
- Bailly, F.; Barthen, P.; Breuer, W.; Frohn, H.-J.; Giesen, M.; Helber, J.; Henkel, G.; Priwitzer, A. *Z. Anorg. Allg. Chem.* **2000**, *626*, 1406.
- Minkwitz, R.; Berkei, M. *Inorg. Chem.* **1998**, *37*, 5247.
- Desiraju, G. R.; Parthasarathy, R. *J. Am. Chem. Soc.* **1989**, *111*, 8725.
- Gavezotti, A. *J. Chem. Theory Comput.* **2005**, *1*, 834.
- Dunitz, J. D.; Gavezotti, A. *Angew. Chem., Int. Ed.* **2005**, *44*, 1766.
- Boese, R. K., M. T.; Dunitz, J. D.; Filippini, G.; Gavezotti, A. *Helv. Chim. Acta* **2001**, *84*, 1561.
- The Desiraju–Parthasarathy analysis of chlorine–chlorine contacts is currently under debate, see refs 38–41.
- Larsen, D. W.; Allred, A. L. *J. Phys. Chem.* **1965**, *69*, 2400.
- Reed, A. E.; Curtiss, L. A.; Weinhold, F. *Chem. Rev.* **1988**, *88*, 899.
- Amoroso, A. J.; Thompson, A. M. W. C.; Maher, J. P.; McCleverty, J. A.; Ward, M. D. *Inorg. Chem.* **1995**, *34*, 4828.
- Frisch, M. J.; Trucks, G. W.; Schlegel, H. B.; Scuseria, G. E.; Robb, M. A.; Cheeseman, J. R.; Montgomery, J. A., Jr.; Vreven, T.; Kudin, K. N.; Burant, J. C.; Millam, J. M.; Iyengar, S. S.; Tomasi, J.; Barone, V.; Mennucci, B.; Cossi, M.; Scalmani, G.; Rega, N.; Petersson, G. A.; Nakatsuji, H.; Hada, M.; Ehara, M.; Toyota, K.; Fukuda, R.; Hasegawa, J.; Ishida, M.; Nakajima, T.; Honda, Y.; Kitao, O.; Nakai, H.; Klene, M.; Li, X.; Knox, J. E.; Hratchian, H. P.; Cross, J. B.; Adamo, C.; Jaramillo, J.; Gomperts, R.; Stratmann, R. E.; Yazyev, O.; Austin, A. J.; Cammi, R.; Pomelli, C.; Ochterski, J. W.; Ayala, P. Y.; Morokuma, K.; Voth, G. A.; Salvador, P.; Dannenberg, J. J.; Zakrzewski, V. G.; Dapprich, S.; Daniels, A. D.; Strain, M. C.; Farkas, O.; Malick, D. K.; Rabuck, A. D.; Raghavachari, K.; Foresman, J. B.; Ortiz, J. V.; Cui, Q.; Baboul, A. G.; Clifford, S.; Cioslowski, J.; Stefanov, B. B.; Liu, G.; Liashenko, A.; Piskorz, P.; Komaromi, I.; Martin, R. L.; Fox, D. J.; Keith, T.; Al-Laham, M. A.; Peng, C. Y.; Nanayakkara, A.; Challacombe, M.; Gill, P. M. W.; Johnson, B.; Chen, W.; Wong, M.; Gonzalez, C.; Pople, J. A. *Gaussian 03*, revision C.01; Gaussian, Inc.: Wallingford, CT, 2004.
- Adamo, C.; Barone, V. *J. Chem. Phys.* **1988**, *108*, 664.
- Perdew, J. P.; Burke, K.; Ernzerhof, M. *Phys. Rev. Lett.* **1996**, *77*, 3865.
- Jensen, F. *J. Chem. Phys.* **2001**, *115*, 9113.
- Dolg, M. In *Modern Methods and Algorithms of Quantum Chemistry*; Grotendorst, J., Ed.; John von Neumann Institute for Computing: Jülich, Germany, 2000; Vol. 1, p 479.

- (51) The set of spd diffuse functions was taken from the SDB-aug-pVTZ basis set.
- (52) Martin, J. M. L.; Bauschlicher, C. W., Jr.; Ricca, A. *Comput. Phys. Commun.* **2001**, *133*, 189.
- (53) Simon, S.; Duran, M.; Dannenberg, J. J. *J. Chem. Phys.* **1996**, *105*, 11024.
- (54) Boys, S. F.; Bernardi, F. *Mol. Phys.* **1970**, *19*, 553.
- (55) Glendening, E. D.; Badenhoop, J. K.; Reed, A. E.; Carpenter, J. E.; Bohmann, J. A.; Morales, C. M.; Weinhold, F. *NBO*, 5.0 ed.; Theoretical Chemistry Institute: University of Wisconsin: Madison, WI, 2001.

CG0607250